Microscopic derivation of a $NN^*(1440)$ potential

B. Juliá-Díaz,[1] F. Fernández,[1] P. González,[2] and A. Valcarce[1]
[1]*Grupo de Física Nuclear, Universidad de Salamanca, E-37008 Salamanca, Spain*
[2]*Departamento de Física Teórica and IFIC, Universidad de Valencia–CSIC, E-46100 Burjassot, Valencia, Spain*
(Received 18 May 2000; published 25 January 2001)

We derive a $NN^*(1440)$ potential from a nonrelativistic quark-quark interaction and a quark cluster model for the baryons. By making use of the Born-Oppenheimer approximation, we examine quark Pauli correlations in detail. A comparison with the NN potential derived in the same framework is done. This makes it possible to emphasize the role of quark antisymmetry beyond baryon antisymmetry and to discuss the use of phenomenological $NN^*(1440)$ baryonic potentials.

DOI: 10.1103/PhysRevC.63.024006 PACS number(s): 12.39.Jh, 13.75.Cs, 14.20.Gk, 24.85.+p

I. INTRODUCTION

The major role played by baryonic resonances has become clear in recent years, in particular the low-lying nucleonic resonances $\Delta(1232)$ and $N^*(1440)$, in many electromagnetic and strong reactions that take place in nucleons and nuclei. This justifies the current experimental effort along this line in several facilities: TJNAF with a specific experimental program of electroexcitation of resonances, WASA in Uppsala to study $NN\to NN\pi\pi$ reactions, etc.

The $\Delta(1232)$ appears as the most important P-wave resonance in the πN system. The $N^*(1440)$ appears as a peak in the (α,α') reaction on a proton target [1] interpreted as an excitation of the target mediated by an isoscalar exchange between the α and the proton [2]. From the point of view of their quark structure the Δ corresponds to a spin-flavor flip of one of the quarks of the nucleon. The quark structure of the Roper resonance seems more elusive. Descriptions as a radial excitation of the nucleon, as assumed in most spectroscopic quark models and which we shall adopt henceforth, are the simplest ones. Alternatively, the Roper resonance has been considered a breathing bag model mode [3] or a hybrid state containing quarks and gluons [4]. Even recently, a possible explanation of the Roper resonance as a dynamical effect in πN scattering has been pointed out without resorting to any quark structure [5].

At the baryonic level, the role played by the Δ in many nucleonic and nuclear reactions has been extensively studied within the framework of the intermediate-energy Δ isobar model [6]. Regarding the $N^*(1440)$ its role in the NN interaction, as much in the scattering problem [7] as in the deuteron structure [8], has been considered in the past. Also the contribution of intermediate $N^*(1440)$ resonances to the three-nucleon interaction has been estimated [9]. More recently, its relevance in $NN\to NN\pi\pi$ reactions has been emphasized [10].

In this context the transition $NN\to NR$ (R is the resonance) and direct $NR\to NR$ and $RR\to RR$ interactions should be understood. Usually these interactions have been written as straightforward extensions of some pieces of the $NN\to NN$ potential with modification of the values of the coupling constants, extracted from their decay widths. Though this procedure can be appropriate for the very-long-range part of the interaction, it is under suspicion at least for the short-range part for which the detailed structure of baryons may determine to some extent the form of the interaction. This turns out to be the case for the $NN\to N\Delta$ and $N\Delta\to N\Delta$ potentials previously analyzed elsewhere [11]. It seems therefore convenient to proceed to a derivation of these potentials based on the more elementary quark-quark interaction. This is the purpose of this article: starting from a quark-quark nonrelativistic potential, we implement the baryon structure through technically simple variational Gaussian wave functions and we calculate the potential at the baryonic level in the static Born-Oppenheimer approach. The $N^*(1440)$, the Roper resonance, is taken as a stable particle. For dynamical applications its width should be implemented through the coupling to the continuum. We center our attention on the $NN^*\to NN^*$ potential where a complete parallelism with the $NN\to NN$ case can be easily established. Notice that the quark-quark interaction parameters are fixed (from the $NN\to NN$ case) and are kept independent of the baryons involved in the interaction. This eliminates the bias introduced in models at the baryonic level by a different choice of effective parameters according to the baryon-baryon interaction considered (this effectiveness of the parameters may hide distinct physical effects).

This article is organized as follows. In Sec. II we revise some details of the NN^* wave function written in terms of quarks. The $NN^*\to NN^*$ potential obtained is showed for different partial waves in Sec. III, where we also discuss its main features. In Sec. IV we discuss the use of phenomenological baryonic $NN^*\to NN^*$ potentials. Finally in Sec. V we summarize our main results and conclusions.

II. NN^* WAVE FUNCTION

In order to describe the NN^* system we shall use a constituent quark cluster model; i.e., baryons are described as clusters of three quarks. Assuming a two-center shell model the wave function of a two-baryon system, B_1 and B_2, with a

definite symmetry under the exchange of the baryon quantum numbers is written [11]

$$\Psi^{ST}_{B_1B_2}(\vec{R}) = \frac{\mathcal{A}}{\sqrt{1+\delta_{B_1B_2}}} \times \sqrt{\frac{1}{2}}\left\{\left[B_1\left(123;-\frac{\vec{R}}{2}\right)B_2\left(456;\frac{\vec{R}}{2}\right)\right]_{ST} + (-1)^f\left\{\left[B_2\left(123;-\frac{\vec{R}}{2}\right)B_1\left(456;\frac{\vec{R}}{2}\right)\right]_{ST}\right\}, \tag{1}$$

$\mathcal{A}$ being the six-quark antisymmetrizer given by

$$\mathcal{A} = \left(1-\sum_{i=1}^{3}\sum_{j=4}^{6}P_{ij}\right)(1-\mathcal{P}), \tag{2}$$

where $\mathcal{P}$ exchanges the three quarks between the two clusters and P_{ij} exchanges quarks i and j.

If one projects on a state of definite orbital angular momentum L, as a result of the $(1-\mathcal{P})$ operator in the antisymmetrizer the wave function $\Psi^{ST}_{B_1B_2}(\vec{R})$ vanishes unless

$$L+S_1+S_2-S+T_1+T_2-T+f=\text{odd}. \tag{3}$$

Since $S_1=\frac{1}{2}=S_2$, $T_1=\frac{1}{2}=T_2$, this fixes the relative phase between the two components of the wave function at Eq. (1) to be

$$f=S+T-L+\text{odd}. \tag{4}$$

It is important to realize that for the NN system f is necessarily even in order to prevent the vanishing of the wave function. No such restriction exists for NN^*. Therefore, there are NN^* channels, f odd, with no counterpart in the NN case. There are however no quark Pauli-blocked channels, i.e., channels where a strong repulsive Pauli hard core is generated. The reason for this absence is that, similarly to the NN case, all the quarks can be accommodated in the same spatial state. Technically, this can be seen by analyzing the normalization of the NN^* wave function. We will assume the three-quark wave function for the quark clusters at a position $\vec{R}$, given by

$$|N\rangle = |[3](0s)^3\rangle, \tag{5}$$

$$|N^*\rangle = \sqrt{\frac{2}{3}}|[3](0s)^2(1s)\rangle - \sqrt{\frac{1}{3}}|[3](0s)(0p)^2\rangle, \tag{6}$$

or more explicitly

$$N(\vec{r}_1,\vec{r}_2,\vec{r}_3;\vec{R}) = \prod_{n=1}^{3}\left(\frac{1}{\pi b^2}\right)^{3/4} e^{-\frac{(\vec{r}_n-\vec{R})^2}{2b^2}} \otimes [3]_{ST}\otimes[1^3]_C \tag{7}$$

and

$$N^*(\vec{r}_1,\vec{r}_2,\vec{r}_3;\vec{R}) = \left(\sqrt{\frac{2}{3}}\phi_1 - \sqrt{\frac{1}{3}}\phi_2\right)\otimes[3]_{ST}\otimes[1^3]_C, \tag{8}$$

where $[3]_{ST}$ and $[1^3]_C$ stand for the spin-isospin and color parts, respectively, and

$$\phi_1 = \frac{\sqrt{2}}{3}\left(\frac{1}{\pi b^2}\right)^{9/4}\sum_{k=1}^{3}\left[\frac{3}{2}-\frac{(\vec{r}_k-\vec{R})^2}{b^2}\right]\prod_{i=1}^{3} e^{-(\vec{r}_i-\vec{R})^2/2b^2}, \tag{9}$$

$$\phi_2 = -\frac{2}{3}\left(\frac{1}{\pi^{9/4}b^{13/2}}\right)\sum_{j<k=1}^{3}(\vec{r}_j-\vec{R})\cdot(\vec{r}_k-\vec{R})\prod_{i=1}^{3} e^{-(\vec{r}_i-\vec{R})^2/2b^2}. \tag{10}$$

Therefore the norm of the NN^* wave function of Eq. (1) can be expressed as

$$\mathcal{N}^{LSTf}_{NN^*}(R) = \mathcal{N}^{Lf}_{di}(R) - C(S,T)\mathcal{N}^{Lf}_{ex}(R), \tag{11}$$

where $\mathcal{N}^{Lf}_{di}(R)$ and $\mathcal{N}^{Lf}_{ex}(R)$ stand for the direct and exchange radial normalizations, respectively, and whose explicit expressions are given in the Appendix. $C(S,T)$ is a factor depending on the total spin (S) and the total isospin (T) of the NN^* system and given by

$$C(S,T) = \frac{1}{4}\sum_{\chi_i=\eta_i=0}^{1}\left\langle\left(\chi_1,\frac{1}{2}\right),\frac{1}{2};\left(\chi_2,\frac{1}{2}\right),\frac{1}{2};S,M_S|P^S_{36}|\left(\chi_3,\frac{1}{2}\right),\frac{1}{2};\left(\chi_4,\frac{1}{2}\right),\frac{1}{2};S,M_S\right\rangle \times\left\langle\left(\eta_1,\frac{1}{2}\right),\frac{1}{2};\left(\eta_2,\frac{1}{2}\right),\frac{1}{2};T,M_T|P^T_{36}|\left(\eta_3,\frac{1}{2}\right),\frac{1}{2};\left(\eta_4,\frac{1}{2}\right),\frac{1}{2};T,M_T\right\rangle, \tag{12}$$

where χ_i (η_i) stand for the coupled spin (isospin) of two quarks. For $L=0$ and $R\to 0$ one obtains

$$\mathcal{N}^{L=0,ST}_{NN^*}(R\to 0)\sim\{1-\tfrac{1}{3}[5+2(-)^f]C(S,T)\}+\mathcal{O}(R^4), \tag{13}$$

where the values of $C(S,T)$ are given in Table I.

TABLE I. $C(S,T)$ spin-isospin coefficients as defined in Eq. (12).

(S,T)	(1,0)	(0,1)	(0,0)	(1,1)
$C(S,T)$	-1/27	-1/27	7/9	31/81

Pauli-blocked channels correspond to $f=$odd and $C(S,T)=1$ or $f=$even and $C(S,T)=3/7$. From the values given in Table I it is clear that although there are no Pauli-blocked channels there is a Pauli repulsion for those S-wave channels without NN counterpart, $(S,T)=(0,0),(1,1)$, i.e., forbidden in the NN case. This is ilustrated in Fig. 1, where we show the norm of the NN^* wave function for $L=0$. As can be seen, the norm gets suppressed in those cases where the channel is forbidden for the NN case. This is a remnant of the near to identity similarity of N and $N^*(1440)$.

III. $NN^* \rightarrow NN^*$ POTENTIAL

To derive the $NN^* \rightarrow NN^*$ potential from a quark-quark interaction we follow the Born-Oppenheimer approximation. We take the potential at the interbaryon distance R as the expectation value of the energy of the six-quark system minus the self-energy of the two clusters:

$$V_{NN^*(L\,S\,T)\rightarrow NN^*(L'\,S'\,T)}(R)=\xi^{L'\,S'\,T}_{L\,S\,T}(R)-\xi^{L'\,S'\,T}_{L\,S\,T}(\infty), \tag{14}$$

where

$$\xi^{L'\,S'\,T}_{L\,S\,T}(R)$$

$$=\frac{\langle\Psi^{L'\,S'\,T}_{NN^*}(\vec{R})|\Sigma^6_{i<j=1}V_{qq}(\vec{r}_{ij})|\Psi^{L\,S\,T}_{NN^*}(\vec{R})\rangle}{\sqrt{\langle\Psi^{L'\,S'\,T}_{NN^*}(\vec{R})|\Psi^{L'\,S'\,T}_{NN^*}(\vec{R})\rangle}\sqrt{\langle\Psi^{L\,S\,T}_{NN^*}(\vec{R})|\Psi^{L\,S\,T}_{NN^*}(\vec{R})\rangle}}. \tag{15}$$

For the quark-quark potential we take a form that has been very much detailed elsewhere [12] and that we write only for completeness:

$$V_{qq}(\vec{r}_{ij})=V_{CON}(\vec{r}_{ij})+V_{OGE}(\vec{r}_{ij})+V_{OPE}(\vec{r}_{ij})+V_{OSE}(\vec{r}_{ij}), \tag{16}$$

where $\vec{r}_{ij}$ is the interquark distance. V_{CON} is the confining potential, whose detailed radial structure is meaningless for the two-baryon interaction. To be consistent with the baryon spectra it will be taken as linear,

$$V_{CON}(\vec{r}_{ij})=-a_c\vec{\lambda}_i\vec{\lambda}_j r_{ij}, \tag{17}$$

where the λ's stand for the color SU(3) matrices. V_{OGE} is the perturbative one-gluon-exchange (OGE) interaction containing Coulombian, spin-spin $(\vec{\sigma}_i\cdot\vec{\sigma}_j)$, and tensor terms (S_{ij}),

$$V_{OGE}(\vec{r}_{ij})=\frac{1}{4}\alpha_s\vec{\lambda}_i\cdot\vec{\lambda}_j \times\left\{\frac{1}{r_{ij}}-\frac{\pi}{m_q^2}\left[1+\frac{2}{3}\vec{\sigma}_i\cdot\vec{\sigma}_j\right] \times\delta(\vec{r}_{ij})-\frac{3}{4m_q^2 r_{ij}^3}S_{ij}\right\}, \tag{18}$$

and V_{OPE} and V_{OSE} are the one-pion-exchange (OPE) and one-sigma-exchange (OSE) interaction given by

$$V_{OPE}(\vec{r}_{ij})=\frac{1}{3}\alpha_{ch}\frac{\Lambda^2}{\Lambda^2-m_\pi^2}m_\pi \times\left\{\left[Y(m_\pi r_{ij})-\frac{\Lambda^3}{m_\pi^3}Y(\Lambda r_{ij})\right]\vec{\sigma}_i\cdot\vec{\sigma}_j +\left[H(m_\pi r_{ij})-\frac{\Lambda^3}{m_\pi^3}H(\Lambda r_{ij})\right]S_{ij}\right\}\vec{\tau}_i\cdot\vec{\tau}_j, \tag{19}$$

$$V_{OSE}(\vec{r}_{ij})=-\alpha_{ch}\frac{4m_q^2}{m_\pi^2}\frac{\Lambda^2}{\Lambda^2-m_\sigma^2}m_\sigma \times\left[Y(m_\sigma r_{ij})-\frac{\Lambda}{m_\sigma}Y(\Lambda r_{ij})\right], \tag{20}$$

where Λ is a cutoff parameter and

$$Y(x)=\frac{e^{-x}}{x}, \tag{21}$$

$$H(x)=\left(1+\frac{3}{x}+\frac{3}{x^2}\right)Y(x). \tag{22}$$

The values chosen for the parameters are the same [12] previously used (they reproduce the experimental values of the πN coupling constant and the $\Delta-N$ mass difference) and are tabulated in Table II.

The Born-Oppenheimer approximation followed integrates out the quark coordinates keeping R fixed. Hence, quantum fluctuations of the two-baryon center of mass are neglected. Nonetheless, we expect that a more complete treatment as the one implied by the use of the resonating group method does not represent, at least for the calculations we perform, major changes as turns out to be the case for the NN interaction [13].

From Eq. (14) and from the structure of the antisymmetrizer the potential contains direct terms, not involving quark exchanges, and quark-exchange pieces. We illustrate in Fig. 2 the most important diagrams contributing to the potential. We have separated them with regards to the part of the radial

TABLE II. Quark model parameters.

m_q (MeV)	313
b (fm)	0.5
α_s	0.4
a_c (MeV fm^{-1})	109.7
α_{ch}	0.027
m_σ (fm^{-1})	3.421
m_π (fm^{-1})	0.70
Λ (fm^{-1})	4.2

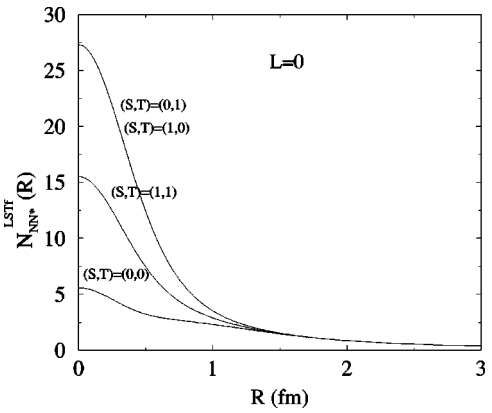

FIG. 1. $NN^*(1440)$ overlapping as a function of the interbaryon distance for $L=0$ partial waves.

wave function that contributes to this diagram. Most of them, diagrams (A1)–(A24), are generated by ϕ_1 [Eq. (9)], diagrams (B1)–(B14) are due to ϕ_2 [Eq. (10)], and the only relevant diagrams coming from the mixing of both terms, ϕ_1 and ϕ_2, are (C1)–(C3). Diagrams (A1)–(A3) and (B1)–(B3) correspond to the self-energy, and are therefore subtracted in Eq. (14). Diagrams (A4), (A5), (B4), and (B5) give the direct contribution, and they generate the asymptotic behavior of the NN^* interaction. The remaining diagrams are of quark-exchange type and their relevance depends on the degree of overlap of the baryon wave functions. Within these, from (A6) to (A13), (B13), and (C3), they correspond to baryon exchange, i.e., $NN^*\rightarrow N^*N$ terms, while the remaining diagrams are associated with $NN^*\rightarrow NN^*$ terms.

Spin-isospin-color matrix elements are the same than in the NN case and can be taken from Ref. [14].

IV. RESULTS

In Fig. 3 we show the potentials obtained for all the $L=0$ partial waves and some representative $L=1$ and $L=2$ partial waves ($T=0$ and $T=1$) as a function of the interbaryon distance. Contributions from the different terms of the potential are also depicted. In Fig. 4 contributions from the different diagrams (for simplicity we have grouped the diagrams attending to their topology; see caption of Fig. 2) are separated for some partial waves.

There are general features of the results for all the partial waves that can be enumerated.

(i) For very long distances ($R>4$ fm) the interaction comes determined by the OPE potential, since this corresponds to the longest-range piece. The OPE is also responsible together with the OSE for the long-range part behavior (1.5 fm $<R<4$ fm), due to the combined effect of shorter range and a bigger strength for the OSE as compared to the OPE.

(ii) For $L=$ even and isospin channels with a correspondence in the NN case, f even, which we shall call *allowed* channels henceforth, the OSE gives the dominant contribution in the intermediate range (0.8 fm $<R<1.5$ fm), determining the attractive character of the potential in this region, analogously for $L=$ odd and *forbidden* channels (those with-

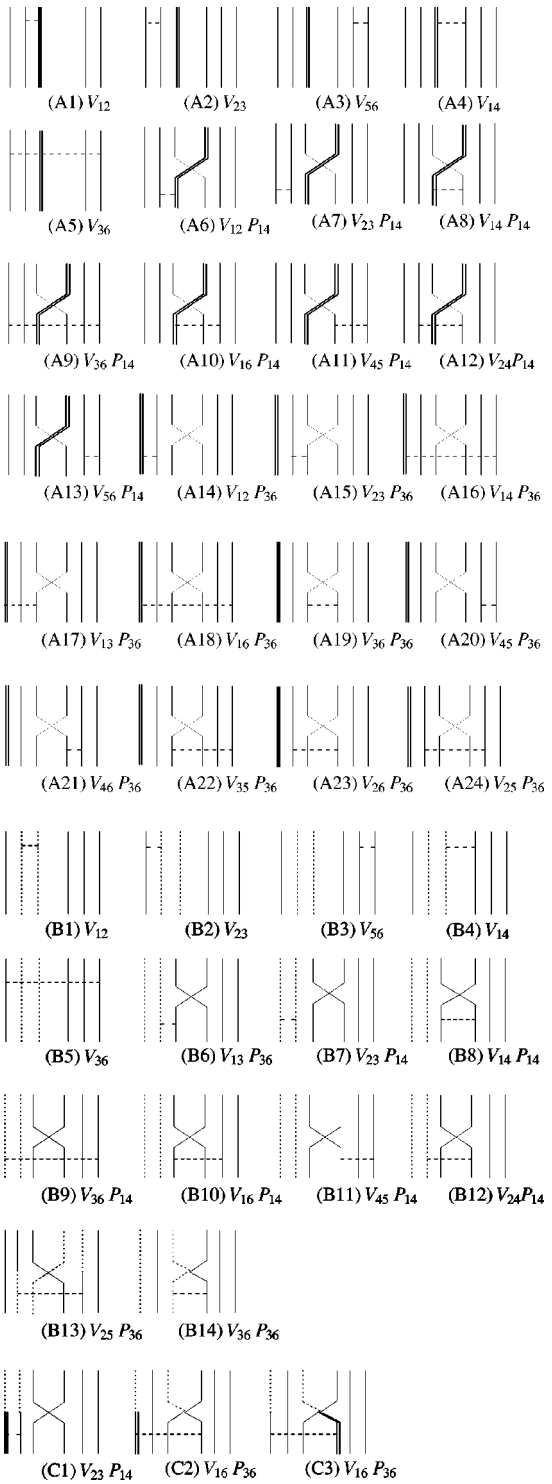

FIG. 2. Different diagrams contributing to the $NN^*(1440)$ interaction. The double line denotes an excited quark on the $1s$ shell and the dotted line stands for an excited quark on the $0p$ shell. Diagrams (A1), (A2), (A3), (B1), (B2), and (B3) are topologically equivalent although involving interactions between excited or non-excited quarks. In the next figures and for simplicity they will be denoted by V_{12}. The remaining diagrams can be also grouped in topologically equivalent classes. The simplified notation in next figures corresponds to such a grouping.

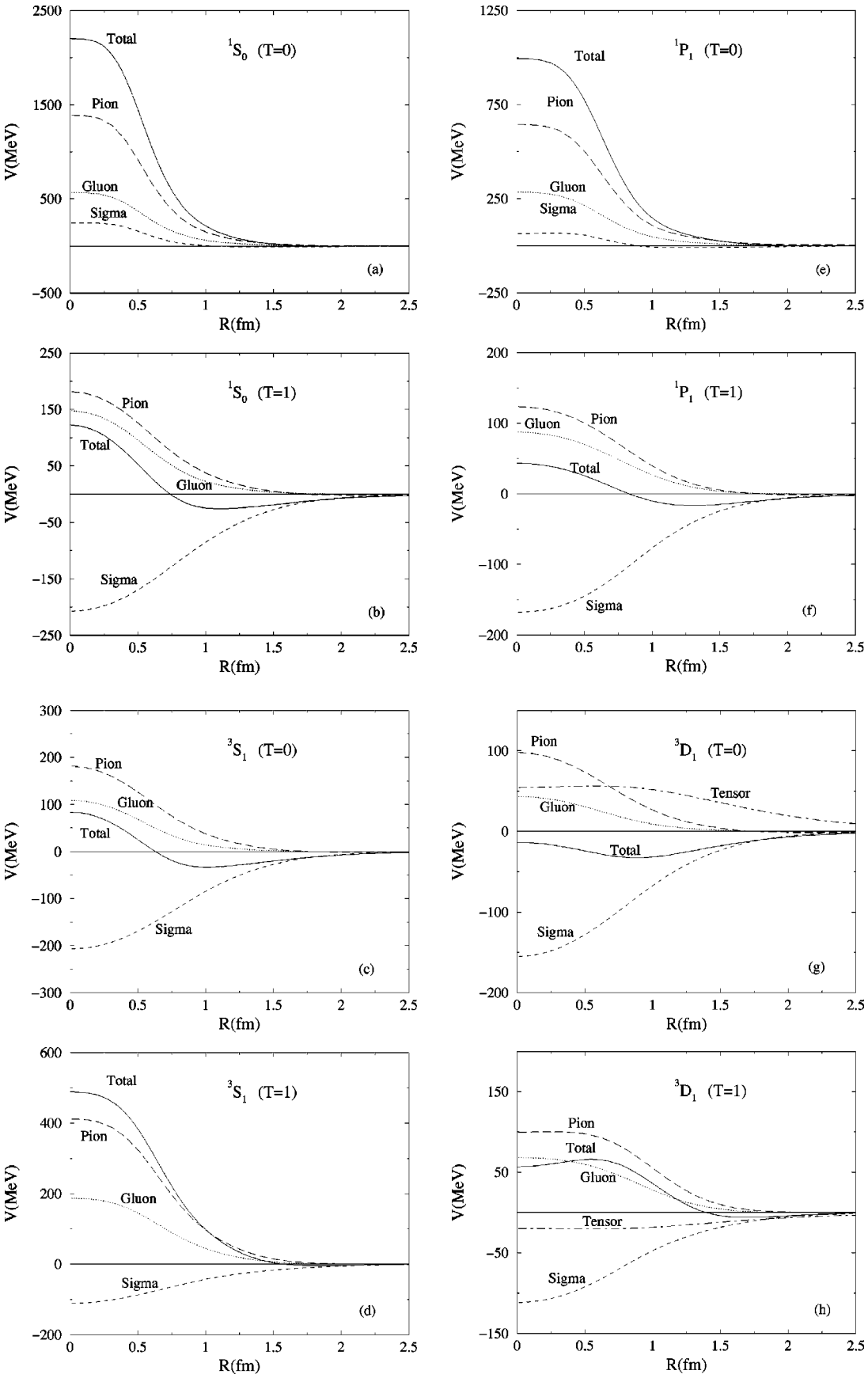

FIG. 3. $NN^*(1440)$ potential for different $L=0,1,2$ partial waves. The contribution of the different terms of the potential has been depicted.

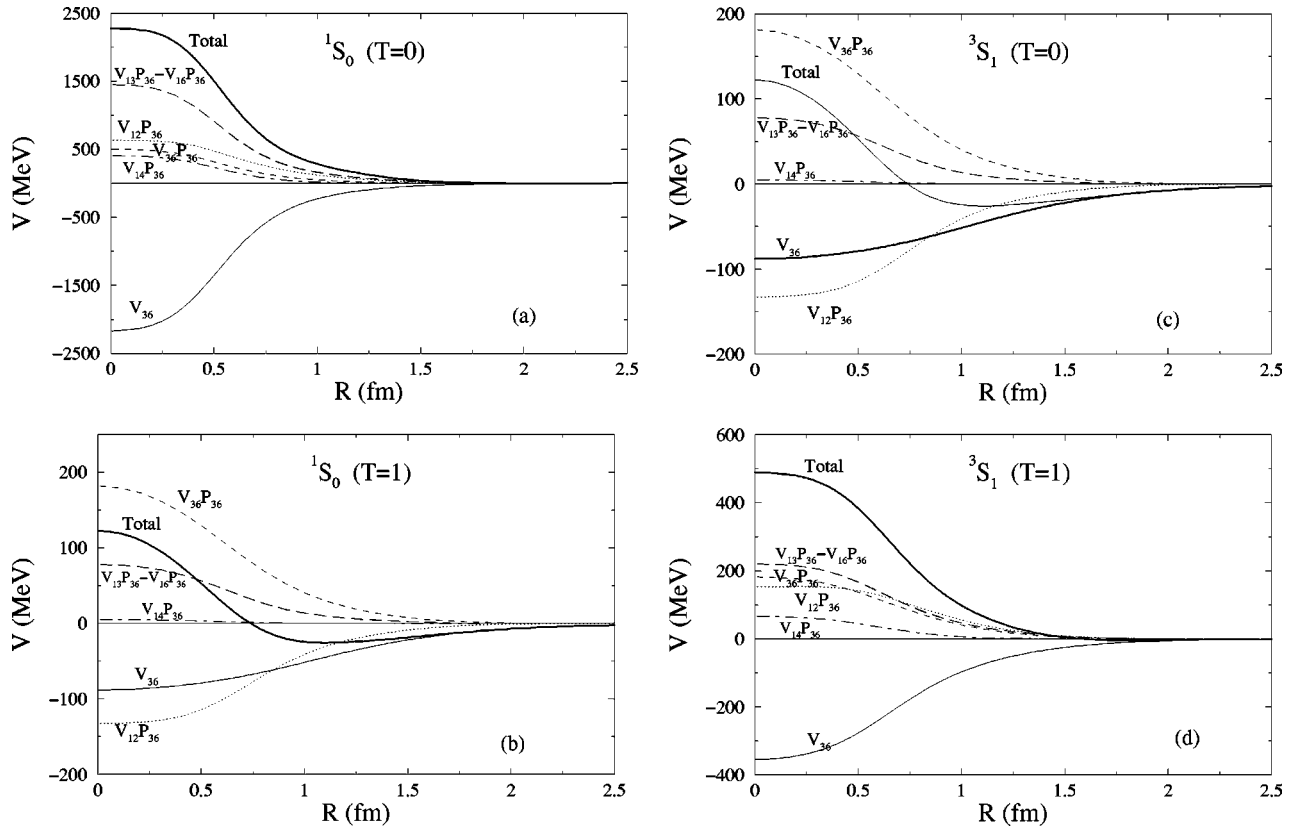

FIG. 4. Same as Fig. 3, but depicting the contribution of the different diagrams drawn in Fig. 2, with the convention explained in the caption.

out correspondence in the *NN* case). In other cases, the OSE reduces its relative contribution or becomes even repulsive. This can be explained by the combined effect of the spatial parity, defined by L, and the spin-isospin parity defined by f. When L and f have the same signature, i.e., when they are both even or odd, the contributions from combinations of the two terms on the right-hand side of Eq. (1) add attractively while for different signature they can alternatively add or subtract.

(iii) For S $(L=0)$ and P $(L=1)$ waves the short-range $(R<0.5$ fm) potential is repulsive. This repulsion comes determined by the OGE and the OPE through quark-exchange diagrams. For D $(L=2)$ waves, where these quark-exchange contributions are weakened by the presence of a stronger centrifugal barrier that prevents a large overlapping of the baryons, the short-range potential may become even attractive [see Fig. 3(g)].

(iv) The *forbidden (allowed)* channels in S and D waves (P waves) are much more repulsive than the *allowed* (*forbidden)* channels. Moreover, the potential for the *forbidden* $^1S_0(T=0)$ channel is very much the same than the potential for the *allowed* $^1P_1(T=0)$ and similarly for $^3S_1(T=1)$ and $^3P_J(T=1)$ (in this last case with small dependences on J due to the tensor interaction). This can be understood in terms of the Pauli and the centrifugal barrier repulsions. The Pauli correlations and the centrifugal barrier in the P waves prevent all the quarks from being in the same spatial state, much the same effect one has due to Pauli correlations in the *S-forbidden* waves added to the presence of the radially excited quark in the $N^*(1440)$.

(v) For the *allowed* (*forbidden)* channels in S or D waves (P waves), the dominant repulsion comes from $V_{36}P_{36}$. This corresponds to the interaction taking place between the same two exchanged quarks. In the other cases, the $V_{13}P_{36}$ or $V_{16}P_{36}$ terms, where an exchanged quark interacts with a nonexchanged one, provide the dominant repulsion. As above, these dominances come from the combined effect, through the P_{36} operator, of the spatial and spin-isospin parities.

(vi) The dynamical effect of quark antisymmetrization can be estimated by comparing the total potential with the one arising from diagram V_{36} which is the only significant one that does not include quark exchanges. The V_{36} potential turns out to be attractive everywhere. Let us note, however, that Pauli correlations are still present in the V_{36} potential, through the norm, in the denominator of Eq. (14). To eliminate the whole effect of quark antisymmetrization one should eliminate quark-Pauli correlations from the norm as well. By proceeding in this way one gets a genuine baryonic potential, which we call the direct potential. Comparison of the total and direct potentials reflects the quark antisymmetrization effect beyond the one-baryon structure. As V_{36}, the direct potential is attractive everywhere (see Fig. 5). It then becomes clear that the repulsive character of the interaction at S and P waves at short distances is due to dynamical quark-exchange effects. For distances $R\geqslant 2$ fm the direct, V_{36}, and

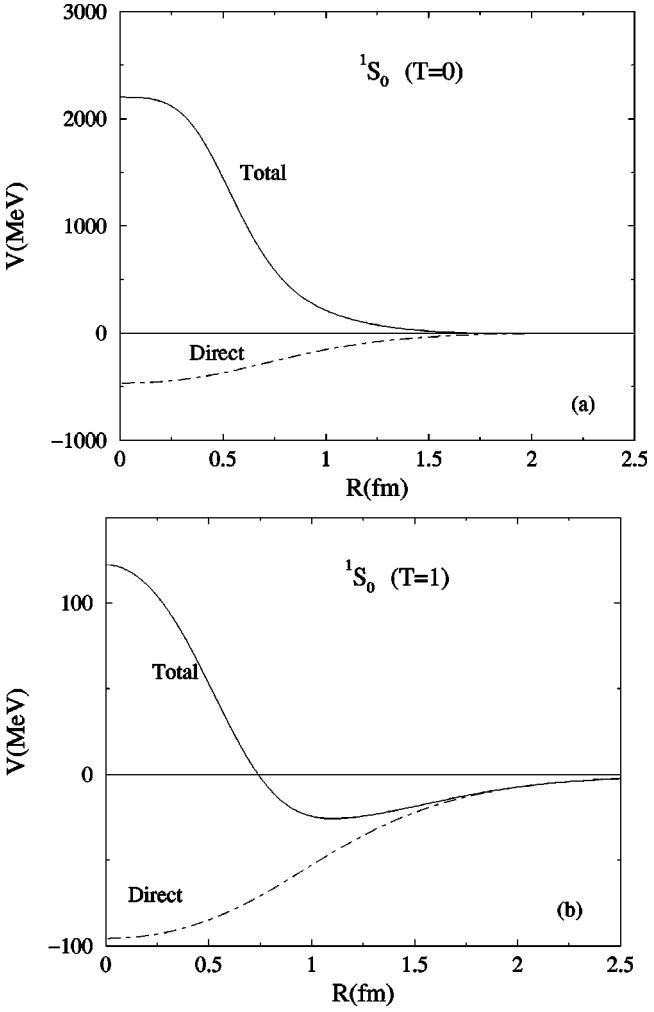

FIG. 5. Comparison between the total and direct (as defined in the text) potential for different $NN^*(1440)$ partial waves.

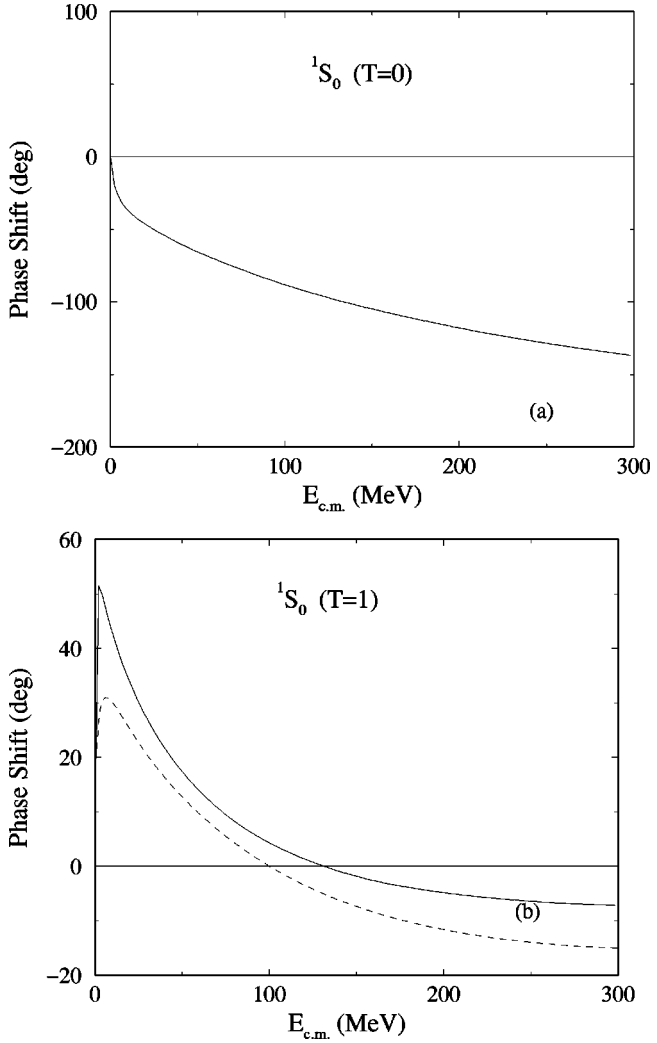

FIG. 6. Phase shifts for $L=0$ $NN^*(1440)$ partial waves (solid line) compared to the corresponding NN phase shifts (dashed line).

total potentials are equal since then the overlap of the N and the $N^*(1440)$ wave functions is negligible and no exchange diagrams contribute appreciably.

(vii) Phase shifts for the two $^1S_0$ isospin channels are shown in Fig. 6. The correlation between *allowed* and *forbidden* states established above translates into values of the corresponding phase shifts. NN phase shifts are also drawn for comparison. The quite similar behavior observed has to do again with the close to identity character of the NN^* and NN wave functions in the *allowed* channels commented on before.

V. PHENOMENOLOGICAL $NN^* \rightarrow NN^*$ POTENTIALS

It is interesting to compare our results for NN^* with the ones obtained for NN derived in the same manner. This will allow us to emphasize the differences derived from the nonidentity of the baryons in the NN^* case and to analyze phenomenological approaches at the baryonic level which take the same form for the $NN^* \rightarrow NN^*$ and the $NN \rightarrow NN$ potentials and proceed to a fit of the strength of the different pieces of the potential from data.

We should first realize that strictly speaking baryonic potentials, for the NN^* case as much as for the NN one, are only justified beyond distances $R \sim 2$ fm, where no quark-exchange effects are present. For $R < 2$ fm the direct potential, which represents a genuine baryonic potential since no quark-exchanges are included, differs very much from the total potential (see Fig. 5). However, we all know the usefulness of effective baryonic potentials where through the parametrization of the form of the interaction and the effective values of the parameters, quark-exchange effects are mostly incorporated. The same seems to be true for *allowed* channels in the NN^* case, since potentials are at most 15% different than NN ones (see Fig. 6).

For *forbidden* states the task of constructing a reliable baryonic potential appears *a priori* more complicated since there is no NN guide. Nevertheless, remembering the discussion in the former section, from the correspondence that can be established between *allowed* and *forbidden* states in different partial waves, one can imagine that a baryonic phenomenological description would also be available.

By proceeding in this way it is important to notice the

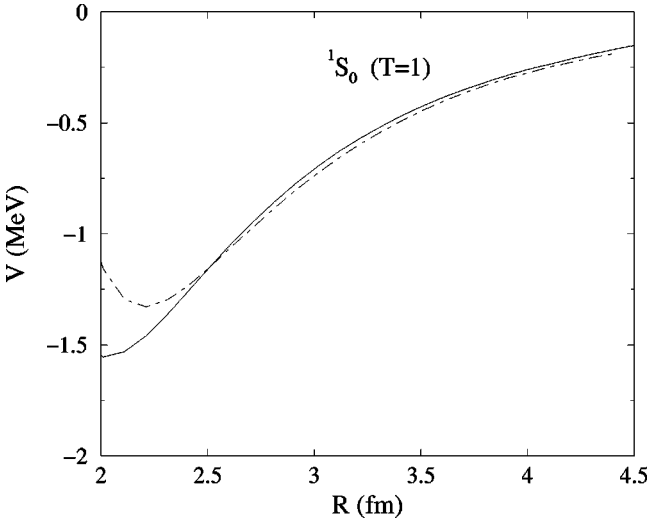

FIG. 7. Asymptotic behavior of the $^1S_0(T=1)$ OPE potential in configuration space for NN (solid line) and $NN^*(1440)$ (dashed line) systems.

main formal difference with the quark treatment related to the fact that quark interaction coupling constants are fixed from NN data once and for all, keeping their values independently of the baryons involved. On the contrary baryon coupling constants are fixed phenomenologically case by case. The same is true for the cutoff masses for the vertices. This makes it possible, at least for some forms of the interaction, to give, from quark coupling values, predictions for the unknown baryonic couplings. Obviously this prediction could be altered in the NN^* case through the inclusion of the N^* width. Let us take for example the OPE potential. Since the pion-baryon-baryon coupling constant is calculated at zero-momentum transfer, we have to examine the asymptotic behavior of the OPE in configuration the baryonic OPE and the quark OPE potential fixes the πqq coupling constant. For NN^* the form of the interaction does not change with respect to NN. Furthermore, as can be checked from Fig. 7 there is no significant difference beyond $R>2.5$ fm between the NN and NN^* cases. One should realize, however, that for NN^*, as a result of the presence of $NN^*\rightarrow NN^*$ as well as $NN^*\rightarrow N^*N$, there are two different couplings involved, $g_{\pi N^*N^*}$ and $g_{\pi NN^*}$, apart from $g_{\pi NN}$. It turns out that the dominant contribution comes from $NN^*\rightarrow NN^*$ from which one concludes that $g_{\pi N^*N^*}\sim g_{\pi NN}$.

Concerning the use of OPE $NN^*\rightarrow NN^*$ potentials, for example in the fitting of the NN scattering at intermediate energies (see, for example, [7]), some caution is necessary. Let us recall that the OPE is the dominant piece only at very long distances, $R>4$ fm. One should be aware that for distances 1.5 fm $<R<4$ fm, the OSE contribution is as important as the OPE. Therefore the use of only the OPE for energies involving long distances might induce an error of the same size as the contribution considered. Certainly this OSE contribution could be to some extent included through a renormalization of the pion-baryon-baryon or of other couplings, but this renormalization depends not only on the particular partial wave but also on energy. Therefore it seems more reliable, when long-range $NN^*\rightarrow NN^*$ potentials are taken into account, for example in NN phase shift analysis for lab energies $T_N\sim 1000$ MeV (N^* threshold), to consider altogether the effects of OPE plus OSE potentials.

For the short- and medium-distance parts of the interaction, the modeling of simple baryonic potentials becomes much more difficult, since quark Pauli effects have nontrivial consequences on the form of the baryonic potential arising from a given form of the quark-quark interaction. This is reflected in phenomenological baryon treatments where quite different forms of repulsive cores are employed to parametrize the interaction. In this respect our results, though obtained in a simple approximation, can serve as a guide for a sensible choice of the parametrization.

VI. SUMMARY

By means of a microscopic quark description of the NN^* interaction we have derived a $NN^*\rightarrow NN^*$ potential. The presence in $N^*(1440)$ of the radially excited quark opens the possibility of having isospin partial waves not allowed in the NN case. *Forbidden* and *allowed* channel potentials have been examined. The strength and range of the different pieces of the quark-quark interaction determine the long-range behavior. For intermediate and short ranges, quark-exchange diagrams together with the dynamics play an essential role as well, determining the attractive or repulsive character of the interaction. The close results obtained for *allowed* channels in the NN^* and the corresponding NN channels contrast with the presence of *forbidden* channels in NN^*. Nonetheless, a correlation of these *forbidden* channels with *allowed* ones in different partial waves can be established, showing in a nice way the equivalence between dynamical and quark Pauli correlations.

The possible use of baryonic NN^* potentials without any explicit quark structure has also been discussed. Our results make clear the difficulties to get sensible parametrizations for all partial waves when no guide from a quark treatment is used and not a sufficient bunch of data is at one's disposal.

Certainly data on $NN^*\rightarrow NN^*$ phase shifts can only be obtained indirectly and no direct experimental test of our results can be performed. Nonetheless, we think our results, at least in a qualitative manner, may help in a better understanding of baryonic processes at a microscopic level and serve as a guide when dealing with reactions where some indicative predictions are needed in theoretical as well as in experimental studies.

ACKNOWLEDGMENTS

This work has been partially funded by Dirección General de Investigación Científica y Técnica (DGICYT) under Contract No. PB97-1401, by Junta de Castilla y León under Contract No. SA-73/98, and by the EC-TMR network under Contract No. TMR X-CT96-0008.

APPENDIX

The explicit expression for the overlapping of the $NN^*(1440)$ wave function given in Eq. (11) is

$$\mathcal{N}_{di}^{Lf}(R)=\left[\frac{2}{3}T_1+\frac{1}{3}T_7+(-)^f\frac{2}{3}T_2\right]$$

$$\mathcal{N}_{ex}^{Lf}(R)=\left[\frac{2}{3}T_3+\frac{1}{3}T_8+(-)^f\frac{2}{3}T_4\right]+2\left[\frac{2}{3}T_5+(-)^f\frac{2}{3}T_6\right], \tag{A1}$$

with

$$T_1=8\pi e^{-\alpha}\left\{ i_L(\alpha)-\frac{R^2}{6b^2}i_L(\alpha)+\frac{R^2}{6b^2}F_1(L,\alpha) + \frac{R^4}{96b^4}i_L(\alpha)-\frac{R^4}{48b^4}F_1(L,\alpha)+\frac{R^4}{96b^4}F_2(L,\alpha)\right\},$$

$$T_2=8\pi e^{-\alpha}\left\{ \frac{R^4}{96b^4}i_L(\alpha)-\frac{R^4}{48b^4}F_1(L,\alpha)+\frac{R^4}{96b^4}F_2(L,\alpha)\right\}, \tag{A2}$$

$$T_3=8\pi e^{-\alpha}\left\{ \frac{R^4}{96b^4}i_L(\beta)+\frac{R^4}{48b^4}F_1(L,\beta)+\frac{R^4}{96b^4}F_2(L,\beta)\right\},$$

$$T_4=8\pi e^{-\alpha}\left\{ i_L(\beta)-\frac{R^2}{6b^2}i_L(\beta)-\frac{R^2}{6b^2}F_1(L,\beta) + \frac{R^4}{96b^4}i_L(\beta)+\frac{R^4}{48b^4}F_1(L,\beta)+\frac{R^4}{96b^4}F_2(L,\beta)\right\},$$

$$T_5=8\pi e^{-\alpha}\left\{ i_L(\beta)-\frac{R^2}{6b^2}i_L(\beta)+\frac{R^2}{6b^2}F_1(L,\beta) + \frac{R^4}{96b^4}i_L(\beta)-\frac{R^4}{48b^4}F_1(L,\beta)+\frac{R^4}{96b^4}F_2(L,\beta)\right\},$$

$$T_6=8\pi e^{-\alpha}\left\{ \frac{R^4}{96b^4}i_L(\beta)-\frac{R^4}{48b^4}F_1(L,\beta)+\frac{R^4}{96b^4}F_2(L,\beta)\right\},$$

$$T_7=8\pi e^{-\alpha}\left\{ i_L(\alpha)-\frac{R^2}{6b^2}i_L(\alpha)+\frac{R^2}{6b^2}F_1(L,\alpha) + \frac{R^4}{48b^4}i_L(\alpha)-\frac{R^4}{24b^4}F_1(L,\alpha)+\frac{R^4}{48b^4}F_2(L,\alpha)\right\},$$

$$T_8=8\pi e^{-\alpha}\left\{ i_L(\beta)-\frac{R^2}{6b^2}i_L(\beta)+\frac{R^2}{6b^2}F_1(L,\beta) + \frac{R^4}{48b^4}i_L(\beta)-\frac{R^4}{24b^4}F_1(L,\beta)+\frac{R^4}{48b^4}F_2(L,\beta)\right\}, \tag{A3}$$

where α and β and the functions F_1 and F_2 are defined by

$$\alpha=\frac{3R^2}{4b^2},$$

$$\beta=\frac{R^2}{4b^2}, \tag{A4}$$

$$F_1(L,x)=\frac{L}{2L+1}i_{L-1}(x)+\frac{L+1}{2L+1}i_{L+1}(x),$$

$$F_2(L,x)=\frac{L(L-1)}{(2L+1)(2L-1)}i_{L-2}(x) + \frac{2L^2+2L-1}{(2L+3)(2L-1)}i_L(x) + \frac{(L+2)(L+1)}{(2L+3)(2L+1)}i_{L+2}(x), \tag{A5}$$

where $i_L(x)$ is the modified spherical Bessel function of the first kind.

[1] H.P. Morsch *et al.*, Phys. Rev. Lett. **69**, 1336 (1992).

[2] S. Hirenzaki, P. Fernández de Cordoba, and E. Oset, Phys. Rev. C **53**, 277 (1996).

[3] G.E. Brown, J.W. Durso, and M.B. Johnson, Nucl. Phys. **A39**, 447 (1983).

[4] T. Barnes and F.E. Close, Phys. Lett. **123B**, 89 (1983); **128B**, 277 (1983); Z. Li, V. Burkert, and Z. Li, Phys. Rev. D **46**, 70 (1992).

[5] C. Shütz *et al.*, Phys. Rev. C **57**, 1464 (1998).

[6] E. Oset, H. Toki, and W. Weise, Phys. Rep. **83**, 282 (1982); E. Oset, in *Proceedings of the International Conference on Mesons and Nuclei at Intermediate Energies*, Dubna, Russia, 1994, edited by M. Kh. Khankhasayev and Zh. B. Kutmanov (World Scientific, Singapore, 1995), p. 569.

[7] E. Lomon, Phys. Rev. D **26**, 576 (1982).

[8] A.M. Green, Rep. Prog. Phys. **39**, 1109 (1976).

[9] K. Shimizu, A. Polls, H. Mütter, and A. Faessler, Nucl. Phys. **A364**, 461 (1981); S.A. Coon, M.T. Peña, and D.O. Riska, Phys. Rev. C **52**, 2925 (1995).

[10] L. Alvarez-Ruso, Phys. Lett. B **452**, 207 (1999).

[11] A. Valcarce, F. Fernández, P. González, and V. Vento, Phys. Rev. C **52**, 38 (1995); A. Valcarce, F. Fernández, and P. González, *ibid.* **56**, 3026 (1997).

[12] F. Fernández, A. Valcarce, U. Straub, and A. Faessler, J. Phys. G **19**, 2013 (1993).

[13] H. Garcilazo, A. Valcarce, and F. Fernández, Phys. Rev. C **60**, 044002 (1999).

[14] A. Valcarce, Ph.D. thesis, University of Salamanca, 1993.